Tailored mesoporous silica nanoparticles for controlled drug delivery: platform fabrication, targeted delivery, and computational design and analysis

Tailored mesoporous silica nanoparticles for controlled drug delivery: platform fabrication, targeted delivery, and computational design and analysis

Xiaodong She[1], Lijue Chen[1], Zhifeng Yi[1], Chengpeng Li[1], Canzhong He[1], Chunfang Feng[1], Tao Wang[2], Sarah Shigdar[2], Wei Duan[2], Lingxue Kong*[1]

1. Deakin University, Geelong, Victoria 3216, Institute for Frontier Materials, Australia
2. Deakin University, Geelong, Vic 3216, School of Medicine, Australia

Correspondence to: Lingxue Kong (E - mail: lingxue.kong@deakin.edu.au)

Abstract:

Mesoporous silica nanoparticles (MSNs) are exceptionally promising drug carriers for controlled drug delivery systems because their morphology, pore structure, pore volume and pore size can be well tailored to obtain certain drug release profiles. Moreover, they possess the ability to specifically transport and deliver anti-cancer drugs when targeting molecules are properly grafted onto their surface. MSNs based drug delivery systems have the potential to revolutionize cancer therapy. This review provides a comprehensive overview of the fabrication, modification of MSNs and their applications in tumour-targeted delivery. In addition, the characterization and analysis of MSNs with computer aided strategies were described. The existing issues and future prospective concerning the applications of MSNs as drug carriers for controlled drug delivery systems were discussed.

Keywords: mesoporous silica nanoparticles, targeted drug delivery, computational design, controlled release

1. Introduction

The synthesis and application of mesoporous silica nanoparticles (MSN) have attracted great attention in the last two decades since the first ordered mesoporous silica molecular sieves (the type of MCM-41) were synthesized by Kresge et al. [1] in 1992. The tunability of their structure including the particle size, pore diameter, and morphology, and the modification and functionalization of surface properties are drawing increasing attention for the purpose of their applications in pharmaceutical [2], optics [3], environmental protection [4] and catalysis [5]. Particularly, as their controllable mesopores (channels) are able to encapsulate pharmaceutical cargoes, the MSNs are exploited to be used as carriers for drug delivery systems.

With the availability of well-established techniques for surface functionalization, MSNs possessing biocompatibility [6] can be selectively modified for specific targeting. MSNs based targeted drug delivery systems were proved to be effective and efficient in killing targeted cell populations. By integrating targeting ligands on the external surface, MSNs can enter and release drugs into cancer cells precisely. In addition, MSNs possess the capacity to level off the drug concentration at the targeted area as the drug molecules are released from the ordered pores or channels of MSNs by a tunable diffusion. When MSNs are functionalized with gatekeepers, burst-release can be effectively prevented, which reduces the dosage and prevents side effects. Furthermore, the large pore volume and large surface areas lead to a higher drug loading [7]. Recent studies have demonstrated examples of MSN as a vehicle for successful intracellular delivery of otherwise poorly soluble or membrane impermeable agents to targeted cells [8].

This review summarizes the key recent developments in the preparation, functionalization and characterization of MSNs for smart delivery, including fabrication mechanism, modifications for targeted and controlled release, accumulation and internalization in cancer cells, calculations and models for MSNs' characterization. This would provide insights into the role of MSNs in the development of nanomedicine.

2. Fabrication of MSNs as nanocarriers

2.1 Formation mechanism of MSNs

There are three key components in the synthesis of MSNs, namely surfactant templates, silica precursors and catalysts. Specifically, the surfactant templates form micelles that evolve mesoporous structure; the silica precursors forms the silica framework outside the micelles; and the catalysts (bases or acids) accelerate the hydrolysis and condensation of silica precursor. The growth mechanism of MSNs has intimate relation to these factors.

The meso-structure is formed after organic surfactants that act as templates are removed [9-11]. A representative synthesis procedure of MCM-41 is shown in Figure 1. The surfactant micelles are first formed in an aqueous solution before the hydrolysed silica source is absorbed on to the micelle surface. MSNs are formed after condensation of silica source and removal of template in mesopores. Experimental conditions, such as the type and concentration of surfactants, system temperature, reaction time and stirring speed, have an impact during the formation of a micelle [12], controlling the pore and particle sizes [13]. An ordered structure of silica shell is then established, the organic templates are eliminated and mesoporous particles are finally obtained. Several general methodologies have been carried out during this process, such as dissolution [14], dialysis [15], and calcination [16]. Nevertheless, with the understanding of the effects of experimental conditions on the mesostructure formation, ideal MSNs can be obtained to fulfil the requirements for drug delivery system.

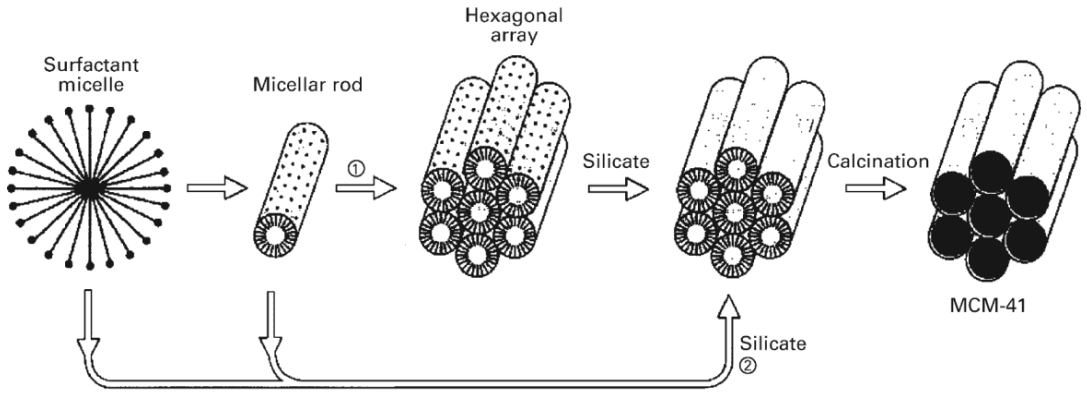

Figure 1 Possible mechanistic pathways for the formation of MCM-41: (1) liquid crystal phase initiated and (2) silicate anion initiated [17].

2.2 Architectural features of MSNs

During the MSN synthesis process, the silicate polymerization directed by templates can be controlled in order to design different architectural features [18]. The morphology of MSNs can be controlled in different ways, including varying templates, controlling the synthesis pH, and choosing additives to control the magnitude of the interactions between the growing silica polymer and the assembled templates. Moreover, the control of the rates of the silica source hydrolysis and condensation is important to attain certain architectural features of MSNs. Sphere, rod, shuttle and lamel are the main structures of MSNs (Figure 2).

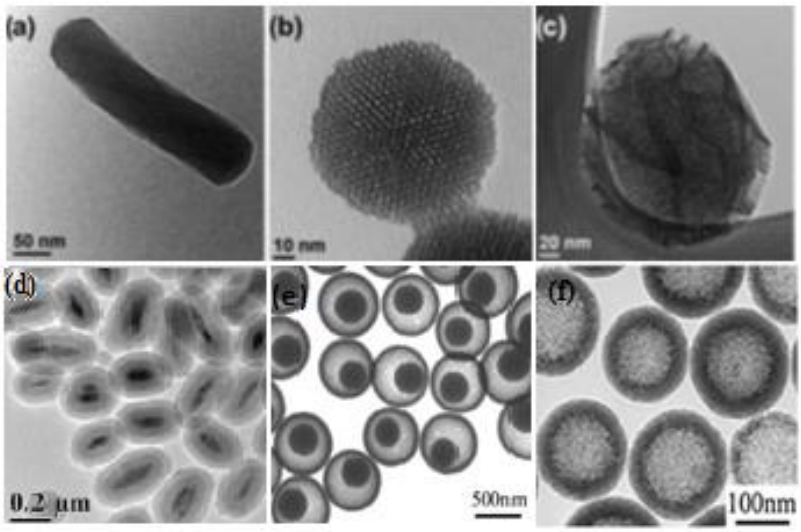

Figure 2 Different particle morphologies of MSNs: (a) rod, (b) sphere, (c) lamel, (d) shuttles, (e) core-shell and (d) hollow particles [7, 19].

Among these MSNs, it is important to choose the right one that can achieve the expected functions. For drug delivery, it was reported that the nanospheres exhibited a higher efficiency of cell internalization when compared with nanorods. This is based on the positive relationship between the particle surface areas and the speed of cell membrane enclosing a particle [20, 21]. Moreover, with the development of nanomedicine, demands for nanoplatforms with specific performance such as large drug loading gradually increase. To meet such new requirements, more and more new methods are under investigation for developing new drug carriers. Hollow MSNs (HMSNs) have been studied as a new-generation drug platform for delivery systems

owning to their extraordinarily high loading capacity. Li and co-workers [22] exploited HMSNs as drug carriers to increase the capacity of storing aspirin.

2.3 Synthesis of hollow MSNs

The formation of meso-structure materials is usually attained by the synthesis of liquid-crystal-like arrays consisting of precursors and templating agents, typically an amphiphilic organic surfactant [13] at low-temperature. For hollow MSN, the synthesis is usually achieved by using a dual template method. More specifically, a hard or soft template (cave template) which is used for the generation of the interior cave is dispersed in a neutral or charged surfactant (pore template). Then pore template micelles are formed around the surface of the cave templating agents. After that, silica matrix coating on the core template is generated by adding silica source agents. Finally, both core and cave templates and pore template micelles are removed by thermal calcination or solvent extraction to obtain hollow MSNs with hollow interiors and mesoporous shells [23].

Soft-templating and hard-templating are typical methods to synthesise HMSNs, where different core templates are utilized for the creation of the hollow cavities [24]. Soft-templating method refers to using surfactants as cave templates to build a hollow interior cave after the removal of surfactants. For example, Feng and co-workers [25] synthesized hollow MSNs through the aggregation of micelles. In their work, (-)-N-dodecyl-N-methylephedrinium bromide (DMEB) was employed as a cave and pore template and carboxyethylsilanetriol sodium salt (CSS) was used to stabilize the DMEB micelles. Importantly, the particle size and mesoporous shell thickness could be changed by altering the pH values during the synthesis possess (Figure 3). It has been suggested that DMEB, CSS and pH values determine the morphology of hollow MSNs. Other surfactants using for hollow MSNs fabrication through soft-templating route include tetrapropylammonium hydroxide [22], hexadecane [26], Pluronic F127 [27] and polystyrene latex [28]. Soft-templating method has been proved to be a simple and effective synthesis approach of hollow MSNs. However, hollow MSNs obtained through this method tend to collapse during the surfactant removing process. Moreover, it is hard to completely remove the cave template through solvent extraction and this in turn will lead to severe side effects when hollow MSNs are used to deliver drugs to human [23].

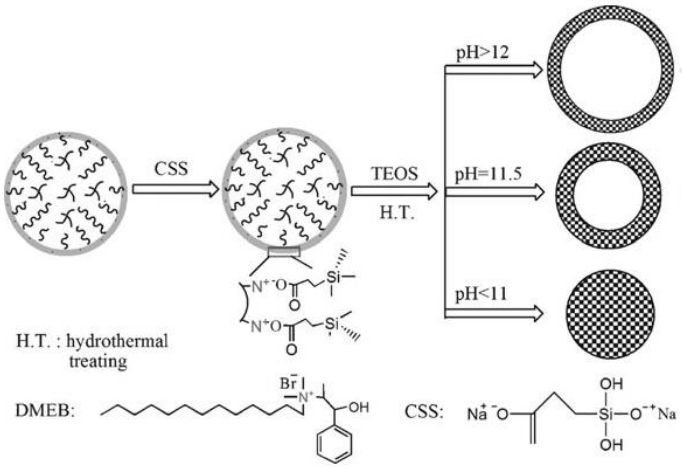

Figure 3 Schematic illustration of the formation process of HMSs [25]

Another strategy for the synthesising of HMSNs relies on employing some solid particles like silica and hematite as hard templates to build a hollow interior cave after template removal process. This fabrication route is made up of four steps: (a) the formation of solid cave templates; (b) core template dispersion. Sometimes functionalization is needed to ensure core surfactants coat the cave templates favourably; (c) silica mesoporous shell generation; and (d) the removal of solid cave. The diameter of the spheres and the caves can be easily tuned by changing the solid core size. Zhang et al [29] prepared hollow MSNs with tunable shell porosity by transforming solid silica particles to hollow structure in NaBH4 solution. Other hard templates being used to create hollow structures are nanospheres of carbon, metals and metal oxides [30]. In general, the challenge of this approach is to fabricate hollow MSNs with small diameters (under 100nm).

Recently, the fabrication of hollow MSNs through select-etching method was developed. Hollow interiors are generated by making use of etching agents to etch the inner cores. This strategy is based on the structural differences or compositional differences between the core and shell structures [31]. Chen et al [19, 31] prepared hollow/rattle-type MSNs by using sodium carbonate solution to etch solid silica nanoparticles, resulting in the building of a hollow cave in the middle (Figure 4). Hollow MSNs were also synthesized with three different pore sizes by a structural difference based selective etching method [32]. In this work, hollow MSNs exhibited the function of controlling drug release rate which was achieved by changing the pore sizes. Similarly, a surface protected approach was developed [33] to prepare hollow MSNs

in which the interior of solid silica spheres was selectively etched by NaOH while their near surface layer was protected by poly (vinyl pyrrolidone).

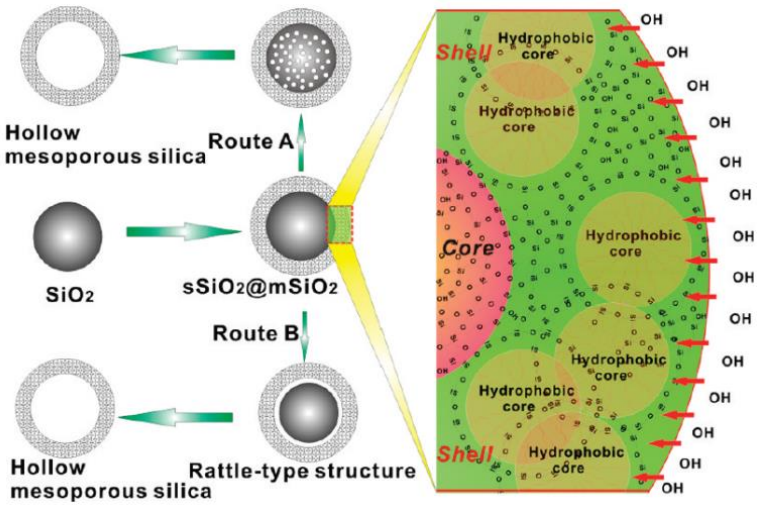

Figure 4 Formation (left) and microscopic structure (right) of hollow/rattle-type MSNs [31]

3. Modification of MSNs for smart delivery

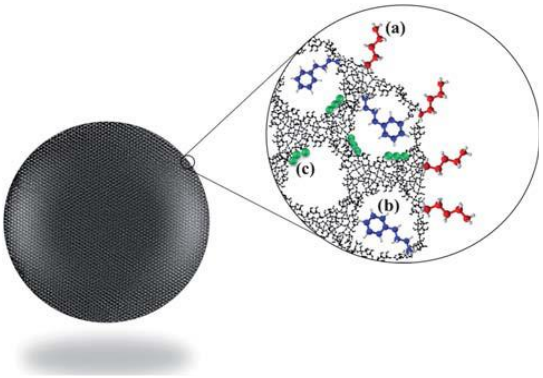

Figure 5 Introduction of functional groups in different regions of MSN, (a) at the external surface, (b) at the pore entrances, or (c) within the walls [7].

After the preparation of MSNs, it is essential that these as synthesized nanocarriers possess designed properties for specific drug delivery systems, such as high cellular uptake, effective cell internalization, higher binding affinity with targeting molecules. In this regard, modification of MSNs is always needed to make MSNs smart carriers for targeting.

As there are many hydroxyl groups existing on the surfaces, MSNs can be modified very easily in different regions, including pore walls, the interior/exterior surfaces and the pore entrance (Figure 5). The introduction of functional groups results in more versatile MSNs. For example, creating hydrophobic and hydrophilic surfaces, and positively and negatively charged surfaces, improving biocompatibility and targeting functions, and regulating drug release rates can be attained by the functionalization of MSNs. He and colleagues [34] changed the surface charge of SBA-15-structured mesoporous silica nanoparticles from -31.1 mV to 29.6 mV by grafting rhodamine B onto the surfaces. Owning to electrostatic attraction, the resulting positively charged MSNs showed an outstanding sustained-release property for a negatively charged drug. The surface of MSNs can be modified with trihydroxysilylpropyl methylphosphonate (THMP) to improve their dispersion [35] as the introduction of THMP on the surface of MSNs increased the electrostatic repulsion between the MSNs and therefore decreased the aggregation.

Methods used for surface modification of MSNs include post synthesis grafting, molecular imprinting, and organosiloxane/siloxane co-condensation. Some functional groups have been widely introduced onto the surface of MSNs through one or more of these methods.

3.1 Surface Modification

Due to the quantum effect of nanosilica, the surface of nanoparticles is covered by tremendous number of active hydroxyl groups. These groups provide potential platform to graft multifunctional polymers onto the surface of external nanoparticles and interior channels. The surface modification creates hydrophobic or hydrophilic surfaces and introduces a unique functional group (C=C, –COOH, or –NH2) onto the surface. The multifunctional grafting focuses on improving biocompatibility, and protecting and controlling the release of guest molecules. The surface modification provides MSNs with multifunction that can facilitate the delivery of biomolecules into cells.

Silane coupling agents are the most commonly used chemicals in surface modification of silica based materials. Reacting with the hydroxyl groups on the surface, the coupling agents can build a bridge that connects organic materials. They also provide a variety of functional groups, such as amine groups, double carbon bonds and epoxy groups (Figure 6). This coupling characteristic as a pre-treatment has been widely utilised to provide the foundation for further modification [36-40]. Also, the functional groups brought by silane modification can introduce different surface properties, such as surface charges and hydrophilicity, which can potentially tune both the capacity of drug loading and the releasing duration [37]. In addition, coupling agents are chemically incorporated on the surface of MSNs so that a successful grafting group is tolerant of physical treatment such as washing, dissolving and stirring.

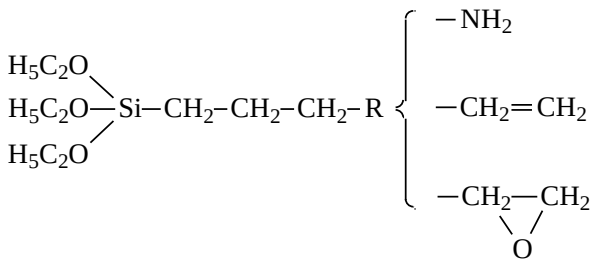

Figure 6 Formulation of silane coupling agents.

3.2 Stimuli-responsive Modification

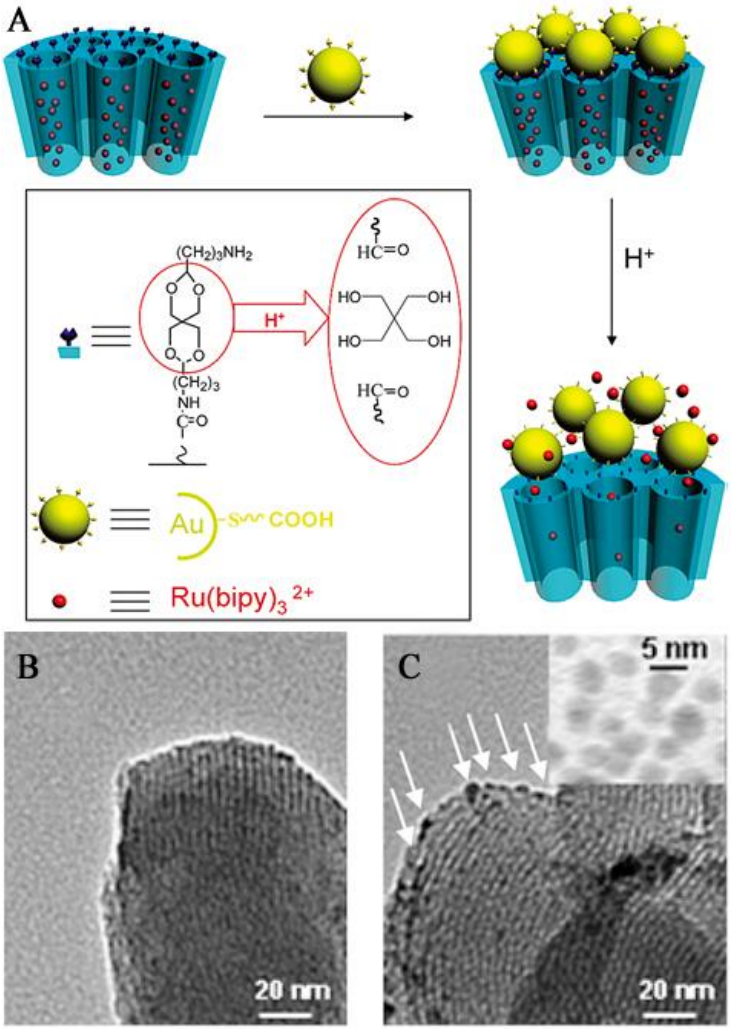

Figure 7 (A) Schematic indication of assembled gold gatekeepers; (B) TEM images of plain MSNs and (C) MSNs with gold nanoparticle gatekeepers at the entrance [41]. Gold nanoparticles are indicated by white arrows in (C).

Various conditions, such as pH value, temperature, magnetism and light, can be used as triggers to release chemicals into the environment [42]. A number of stimuli-responsive protectors have been developed to achieve controlled release. Due to specific porous structure of MSNs, most stimuli-responsive functionalization happens through gatekeepers at the entrance of the channels (namely mesopores). Gold (Au) nanoparticles are the most commonly used medium for this purpose. Au nanoparticles and MSNs can be connected with pH sensitive polymers [41, 43]. In neutral conditions, guest molecules are blocked in the channels of MSNs. The results show that the gold gatekeepers are located at the end of mesopore channels (Figure 7 C) under electron microscope after assembly onto the raw MSNs (Figure 7 B). When the surrounding

pH becomes acidic, the hydrolysis of acetal groups allows the gates blocked by gold to be open, leading to the release of entrapped molecules (Figure 7 A). For the redox-responsive release, cadmium sulfide nanoparticles (CdS) nanoparticles and organic molecules have been implemented to protect guest molecules in MSNs, based on the theory of conditional stimulation [44-46]. The light mediated release of loaded cargos is related to the light sensitive materials, such as gold nanorods [47, 48] and rare element particles [49], which can maintain the loaded molecules in mesopores and responsively release them with an external light source. However, because the main compositions of these gatekeepers are heavy metals that have adverse effects on plant cells and tissues after breaking away from MSNs, the potential use of these types of nano gatekeepers must be carefully examined. A recent study suggested that short-chain molecules can be used as redox-responsive gatekeepers to control the release of a plant hormone – salicylic acid (SA) [50]. The toxicity issue brought by metal gatekeepers can be minimised by this new gatekeeper system. The short-chain molecules were grafted on MSNs with disulfide bonds, and glutathione (GSH), an endogeneous protein, can trigger the cleavage of disulfide bonds, which induce the release of loaded biomolecules (Figure 8). The results from in vitro release showed the GSH concentration dependent release patterns. This GSH mediated release of SA has also been tested in vivo, which indicates the continuous expression of pathogen resistant gene (PR-1) for up to 7 days compared to the short expression of PR-1 with bare SA treatment.

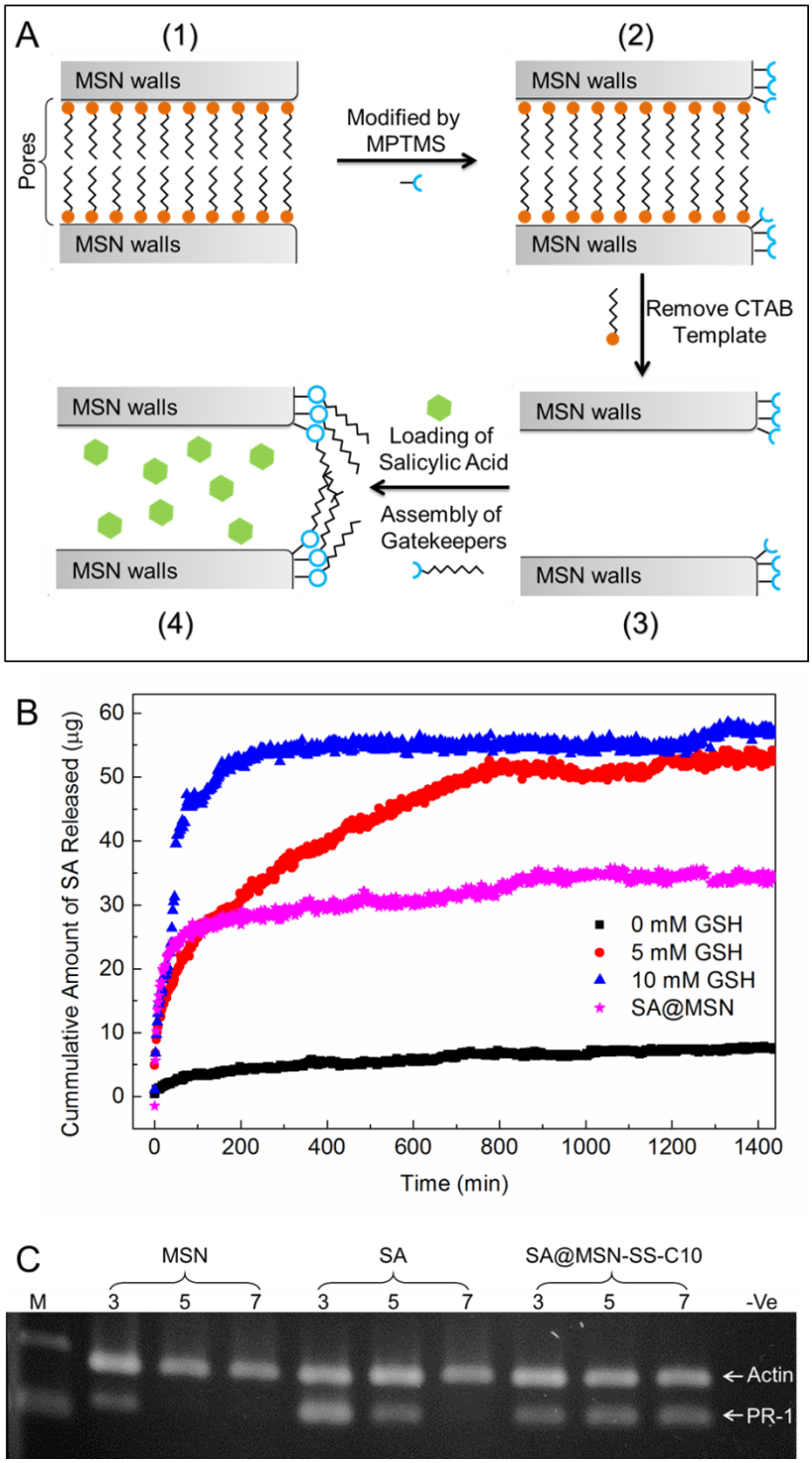

Figure 8 (A) Schematic of functionalization of MSNs with thiol (-SH) groups and assembly of gatekeepers on to SA loaded MSNs. (B) Cumulative amount of SA released from short-chain molecule capped MSNs under different GSH concentration. (C) Housekeeping gene actin and defence gene (*PR-1*) expression in *Arabidopsis* with MSN, SA and SA loaded and capped

MSNs (SA@MSN-SS-C10) treatment on day 3, 5 and 7. M is HyperLadder^{TM} IV (Bioline) and -Ve is the blank channel. Actin is at the top row and PR-1 is at the bottom row.

3.3 Biocompatible polymeric coating

Biocompatible polymeric coatings can potentially enhance the permeability and retention, due to the improvement in biocompatibility. PEGylation is a representative technique that can achieve homogeneous particle dispersion and particularly reinforce the permeability of MSNs across the cell membrane. Several biocompatible materials have been used to coat onto the surface of MSNs, including PEG (poly(ethylene glycol)) [51] and TEG (triethylene glycol) [43]. After MSNs are PEGylated, it is obvious from the confocal microscopy images (Figure 9) that the modified MSNs have more chance to be internalised into cells [51].

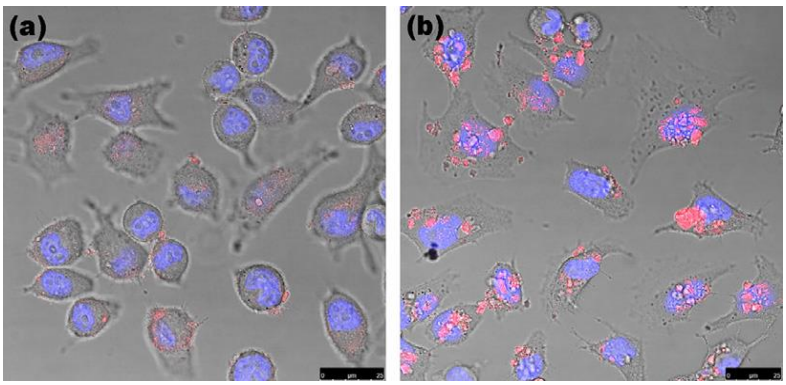

Figure 9 Distribution of hollow sphere mesoporous silica (HSMS) in Hela cells. (a) HSMS with fluorescent agents; (b) HSMS-PEG with fluorescent agents [51]. The cell nuclei are in blue and nanoparticles are in red.

In addition to the enhancement in permeability, the release kinetics of loaded molecules can be manipulated by the polymeric coatings with different thicknesses. Niu et al. [52] prepared core-shell mesoporous silica spheres with controllable shells with a thickness of 5 nm, 25 nm and 60 nm, respectively. The shell is also formed by mesoporous silica and can have different pore size. Due to the size gradient of mesopores, chemicals loaded inside can be gradually released according to the thickness of the shell. The results showed that the thicker the shell coatings

are, the longer the release takes (Figure 10). This methodology indicates another prospect of the controlled drug delivery systems.

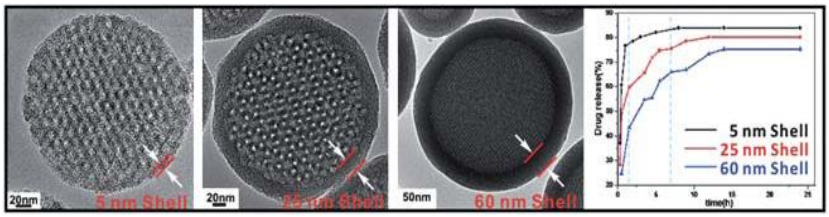

Figure 10 Different shells with different release rate of drugs [52]. The TEM images (left three figures) show the core shell structure of MSNs, and the release kinetics (right graph) show the difference of release duration.

4 Targeted drug and gene delivery

4.1 Accumulation of MSNs in tumour via EPR effect

Various methods have been used to fabricate MSNs with different features that are favourable for drug loading, release and intracellular delivery. Most of them were designed to achieve passive tumour targeting via enhanced permeability and retention (EPR) effect as this is the principle mechanism for nanoparticles to accumulate in tumour site after intravenous injection [53]. With more stable structure compared to biodegradable nanocarriers, MSNs are supposed to maintain their formation in the circulation for longer time and protect the cargoes from premature release. The study of biodistribution of MSNs in live animals should be necessary before the drug loaded MSNs can be used in human body and the data from this study will be invaluable to improve the effect of MSNs on targeted drug delivery.

Many researchers have studied the biodistribution of MSNs in tumour bearing mice to investigate their tumour accumulation by "EPR" effect. Lu et al. prepared folic acid (FA) grafted MSNs with particle size of 100-130 nm and investigated the biodistritubtion in nude mice bearing subcutaneous MCF-7 xenografts [6]. The accumulation of MSNs with or without folic acid in the tumours can be detected by the fluorescent labelling on the particles 4 and 24 h post injection. The quantitative measurement of MSNs and FA-MSNs in tissues was achieved by detecting silica amount 4, 24 and 48 hours post injection using ICP-MS. The tumours in mice treated with MSNs were found to have higher silica concentration than other organs, which can be attributed to the passive tumour targeting "EPR" effect. The active targeting effect of folic acid on MSNs was demonstrated by the enhanced FA-MSNs accumulation in tumour compared to MSNs. Similar result can be seen in the study conducted by Mamaeva and co-worker [54] that folate-tagged MSNs remained in tumour with longer time than MSNs without folate. This phenomenon can be explained by the higher cellular uptake of folate-tagged MSNs compared to MSNs without folate because of the targeting capability of folic acid. As the MSNs can be preferably taken in tumour xenograft, they should be able to bring

anti-cancer drugs in tumour cells. This hypothesis can be demonstrated by detecting the drug concentration in the tumours after intravenous injection of drug loaded MSNs. Similarly DOX was loaded onto MSNs to overcome multidrug resistance in cancer cells in vitro and in vivo [55]. The biodistribution of DOX was investigated after intravenous injection of DOX-MSNs. The results showed that the mice treated with DOX-MSNs had higher DOX concentration in tumour than that of mice treated with free DOX. This study confirmed the different mechanisms of DOX in MSNs and free DOX accumulating in tumours.

Based on these progresses on understanding the biodistribution of MSNs in vivo, other efforts have been made to optimise the targeting effect of MSNs by changing their properties. With smaller size and modified surface with polymers, particle opsonisation of MSNs can be reduced with better monodispersion and tumour accumulation. After intravenous injection of 50 nm doxorubicin-loaded MSNs grafted with polyethyleneimine-polyethylene glycol copolymer in tumour bearing nude mice, around 12% of injected MSNs can be detected in tumour site with high internalization of DOX in KB-31 cells. At the same time, the anti-tumour effect of DOX loaded in MSNs was enhanced with less systematic side effect as compared with free DOX [56]. Chen et al. investigated the biodistribution of TRC105 (an antibody binds to CD105) conjugated HMSN in the mice with breast cancer and found the tumour accumulation of injected particles in mice treated with TRC105-HMSNs was 10% ID/g, which was 3 times higher than that in mice treated with HMSNs without TRC105 [57]. With their superior tumour accumulation due to passive EPR effect and active targeting agent grafted on the surface, MSNs have also been explored as in vivo PET imaging agent, which can be achieved by labelling MSNs with radioactive element [58-60]. As such, MSNs tend to be explored as theranostic nanomedicine that acts as both imaging agent for tumour diagnosis and nanocarriers for cancer drug delivery. Chen et al. [61] developed MSNs based theranostic nanoparticles for cancer management. Copper sulfide (CuS) nanoparticles were encapsulated in the core of MSNs as imaging agent owing to their near-infrared fluorescent absorption. The CuS@MSN was also labelled with copper-64 for biodistribution study by PET imaging. The surface of MSNs was modified with PEG and TRC105 for better biodistribution and active tumour targeting. The biodistribution study in tumour bearing mice reveal that 64Cu-CuS@MSN-TRC105 can be highly taken in tumour site, which makes the MSNs a promising theranostic nanomedicine for future cancer management [61].

From those biodistribution studies on the tumour bearing mice, the liver and spleen can be found to have high accumulation of MSNs. The biodistribution study of MSNs in mice without tumour have also revealed this phenomenon. Liu and co-workers [62] studied the silicon content in different organs by inductively coupled plasma-optical emission spectrometer (ICP–OES) after intravenous injection of 80 mg/kg of MSNs in healthy mice. MSNs in liver and spleen can reach the peak at 24 h with 85% of the injected MSNs. The level of MSNs in liver and spleen decreased after 24 hours and can be detected within 4 weeks. This study suggested that MSNs have long circulation time in the body and can be excreted from reticuloendothelial system (RES) in liver and spleen, in which the MSNs will be taken by macrophages. PEG was often grafted on the surface of MSNs to improve their dispersity and performance in vivo, as demonstrated by He et al [63] that the PEGylated MSNs were able to escape RES and tended to have longer blood-circulation lifetime with slower renal clearance rate. The effects of different factors such as shape [64], size [56, 63], charge [65, 66], and porosity [67] on MSNs biodistribution have also been investigated. All these approaches were intended to increase the circulation time of MSNs in the body and decrease their accumulation in the RES so that the MSNs would have a higher chance to accumulate in tumour site by EPR effect.

4.2 Internalization of MSNs in cancer cells

When the MSNs reach the tumour site through circulation, they are supposed to deliver anti-cancer drugs in tumour cells. Ideal MSNs should be able to enter target cells and release drugs intracellularly. The most important barrier that blocks MSNs from uptake by target cells is the cell membrane. Large particles cannot penetrate the cell membrane; they are internalized into cells mainly by endocytosis [68]. Endocytosis is a process in which particles first interact with the cell surface, become wrapped by the cell membrane and are invaginated, then the vesicles form to enclose the particles and transfer them to endosomes and lysosomes [69]. There are several different types of endocytosis, such as phagocytosis, macropinocytosis, clathrin-mediated, caveline dependent and receptor-mediated endocytosis [70]. Slowing and co-workers [71] studied the endocytosis mechanism of MSNs capped with poly (amidoamine) (PAMAM) dendrimer (PAMAM-MSNs) in Hela cells. Using specific endocytic trafficking inhibitors, they demonstrated that the uptake of MSNs occurred via a clathrin-dependent endocytosis mechanism. The endocytic process of MSNs could also be monitored using differential interference contrast microscopy and different steps related to endocytosis

including Brownian motion in the cell, being trapped on the cell membrane and formation of vesicle in cytoplasm had been observed during the process of MSNs internalization in human lung cancer cells [72]. The endocytosis of MSNs in MDA-MB-468 cells was confirmed as the MSNs were observed to be co-localized with lysosomes [73]. Hollow MSNs could enter cells in a similar endocytic mechanism [74].

The particle size of MSNs may affect their internalization in cells. MSNs with different sizes (30, 50, 110, 170, and 280 nm) were fabricated and the influence of particle size on cellular uptake in Hela cells was investigated [75]. They found that MSNs of 50 nm are the most favourable size for efficient internalization in Hela cells. To examine the internalization of MSNs in MC3T3-E1 cells, MSNs with particle size ranging from 55 nm to 440 nm were fabricated . In vitro result suggested that MSNs with particle size around 100 nm had highest cellular uptake rate [76]. Ekkapongpisit et al. found that the MSNs with the particle size of 10 nm and 50 nm were both internalized in ovarian cancer cells via caveolae-mediated endocytosis. However, the 50 nm MSNs was observed to be resided within lysosomes while the 10 nm ones can escape from endo-lysosomes and enter the cytoplasm [77]. Thus the MSNs of smaller size may have better performance on intracellular delivery of drugs to cytoplasm. The “ultrasmall” small hollow MSNs with a size of 24.7 nm have been demonstrated to have better endocytosis properties in HeLa cells compared to conventional and larger mesoporous silica nanoparticles [78].

There are many other factors that can also influence the uptake of MSNs in cells including the surface charge, shape and structure. Since the cell membrane harbours negative charge on the surface, it is believed that MSNs with a positive charge can be internalized more efficiently than MSNs with a negative charge. The effect of the surface charge on MSNs cellular uptake in hMSCs and 3T3-L1 cells was investigated [79] and it was found that positively charged MSNs have a higher internalization rate in 3T3-L1 cells compared to MSNs with negative charge. However this was not found in hMSCs cells, suggesting that the effect of charge could be cell dependent. The study from Ekkapongpisit et al. revealed that the MSNs with positive charge had higher cellular uptake rate in in ovarian cancer than MSNs with negative charge [77]. Another study reported MSNs grafted with cationic liposomes Lipofectamine 2000 had

higher cellular uptake rate than that of naked MSNs with negative surface charge, which confirmed the charge effect on the endocytosis of MSNs [80].

The shape of MSNs can also affect their internalization rate in cells. Trewyn et al. investigated cellular uptake of both spherical and tube-shaped MSNs in human fibroblast cells [81]. The endocytic rate of spherical MSNs was significantly higher than that of rod-like MSNs, which could be explained by the theory of "wrapping time" that it may take longer time to wrap a rod shape particle than a sphere because of the larger surface area [82]. However, the study on the effect of shape on MSNs cellular uptake by Huang et al. obtained an opposite result: MSNs with largest aspect ratio exhibited highest cellular uptake rate [83]. A different mechanism was introduced to interpret the data: rod shape MSNs have larger contact area with the cell membrane than spherical ones which is more favourable for cellular uptake. More studies should be conducted to confirm the shape effect on MSNs cellular uptake in the future.

The enhanced uptake of MSNs can be achieved by surface modification with targeting molecules [84]. Recently, MSNs have been conjugated with various ligands recognizable by receptors on the cell membrane to achieve active targeted drug delivery via receptor-mediated endocytosis. Folic acid have been frequently used as targeting ligand for various nanocarriers due to the overexpression of folate receptor on most cancer cells. Since it was reported that folic acid on polyethylene imine (PEI) coated MSNs could facilitate their cellular uptake via a receptor-mediated endocytosis [85], folic acid has been grafted on MSNs as effective targeting agent to deliver various therapeutic cargoes into different cancer cells [86-90]. Many other studies attached hyaluronic acid on the MSNs surface to target CD44 overexpressed cancer cells [91-95].

Epidermal growth factor receptor (EGFR) have been found overexpressed in most cancer cells and could be explored as biomarkers for active targeting of nanocarriers. It was found that epidermal growth factor receptor antibody (EGFRAb) conjugated MSNs had superior cellular uptake rate in lung cancer cells compared to normal lung cells due to the overexpression of EGFR in lung cancer cells that can facilitate the receptor-mediated endocytosis of EGFRAb-MSNs [96]. Recently, EGF was grafted on the surface of hollow MSNs to target EGFR on

colorectal cancer cells. The amount of EGF on the surface of HMSNs can be controlled and determined by time of flight secondary ion mass spectrometry (ToF-SIMS) [97] and specific internalization of HMSNs in colorectal cancer cells can be achieved via EGF-EGFR mediated endocytosis with high 5-FU intracellular release to overcome drug resistance [98, 99].

4.3 Delivery of siRNA by MSNs for gene therapy

Since the double-stranded RNA (dsRNA) was first demonstrated to have RNA interference (RNAi) effect in 1998 by Fire and his colleges [100], this technology has been widely used to knock down pathological gene expression for treatment. After internalized into cells, dsRNA can be recognized by the enzyme Dicer and cleaved to short interfering RNA (siRNA). siRNA is then loaded into RNA-induced silencing complex (RISC), the double strand of RNA will be separated in RISC, and the guide strand that is complementary to the mRNA sequence can be hybridized to mRNA and cause the gene silencing by targeted mRNA cleavage [101]. Using this technology, gene therapy that silences certain genes can be promising for diseases such as cancer in which upregulation of certain gene expression can be identified. As for drug resistance in cancer, there are various mechanisms involved including pump and non-pump resistance. Some transmembrane proteins have been identified such as P-glycoprotein (Pgp) which can act as drug efflux pump [102]. Besides Pgp, other factors that influence apoptosis, DNA damage repair or drug metabolism can also play an important role in drug resistance. Furthermore, due to different drugs being used in cancer therapy, the mechanism of drug resistance may be different. After identification of specific genes or proteins that regulate drug resistance, siRNA can be used to knock down those genes to retain drug sensitivity. With the stable porous structure, tuneable size, high loading efficiency and large surface area for chemical modification, MSNs can be a suitable vector for co-delivery of anti-tumour drugs and siRNA to overcome drug resistance.

Due to their mesoporous structure, the MSNs have large surface area that can be grafted with various functional groups that are favourable for drug and siRNA loading. Taking advantage of the negative charge on siRNA, MSNs can be functionalized with positively charged links to attract siRNA by charge effect. Polyethyleneimine (PEI) polymers were grafted on the MSNs to generate a cationic surface to which siRNA can be attached. The effective siRNA delivery by PEI functionalized MSNs was demonstrated by the successful gene knocking down of GFP

expression [103]. Then the PEI-MSNs were used for co-delivery of doxorubicin (Dox) and P-glycoprotein (Pgp) siRNA to KB-V1 cells for overcoming the drug efflux pump mediated multiple drug resistance (MDR). The effective delivery of siRNA by PEI-MSNs can silence the Pgp expression in KB-V1 cells and restore the sensitivity of cells to Dox [104]. This system was then functionalized with PEG for in vivo tumour siRNA delivery via EPR effect. The results demonstrated that siRNA and Dox co-delivered with MSNs can cause effective tumour biodistribution and lead to synergistic inhibition of tumour growth in vivo with significant Pgp gene knockdown [105]. PEI has been frequently used in MSNs based siRNA delivery system as effective coating for siRNA attachment [106-111].

However, the cytotoxicity of PEI may limit its application in vivo. Chen and co-workers modified MSNs with cationic generation 2 (G2) amine-terminated polyamidoamine (PAMAM) to absorb B-cell lymphoma 2 (Bcl-2) siRNA and co-deliver Dox into multidrug resistant A2780/AD human ovarian cancer cells. This siRNA co-delivery system was demonstrated to be capable of silencing Bcl-2 mRNA and enhancing cytotoxicity of Dox [112]. Other types of cationic polymers such as poly(2-(diethylamino)ethylmethacrylate) (PDEAEMA) [113], poly-L-lysine (PLL) [114] and poly(2-(dimethylamino)ethylmethacrylate) (PDMAEMA) [113] have also been used in MSNs based siRNA delivery system with effective siRNA loading and intracellular delivery to cause gene silence.

In most of the above studies, siRNA were attached to the cationic polymers on the MSNs surface through electrostatic interaction. Thus the amount of siRNA loaded on MSNs may be limited if the space within the mesopores of MSNs cannot be utilized. Li and co-workers [115] packaged Bcl-2 siRNA into the mesopores of magnetic MSNs under a strong dehydrated solution conditions. The siRNA loaded MSNs were then grafted with PEI to protect siRNA from premature release. This siRNA loaded MSNs can be internalized into cancer cells and release siRNA to silence Bcl-2 genes. By grafting a fusogenic peptide (KALA**)** on the surface of MSNs, the active targeting effect of this siRNA delivery system was achieved [109]. Furthermore, this siRNA delivery system was functionalized with PEG and systematically administrated in tumour bearing mice with effective vascular endothelial growth factor (VEGF) gene silencing in vivo [116, 117]. Another effective way of increasing the siRNA loading in mesopores that have been demonstrated is to expand the pore size and pore volume for more

siRNA to enter the pores. MSNs with large cubic pores (13.4 nm) functionalized with poly-L-lysine (PLL) were prepared for gene delivery applications; this system was able to carry siRNA with high efficiency and cause specific gene silence [114]. Another study demonstrated that MSNs with ultra large pores (23 nm) was able to load much more siRNA as compared with MSNs with regular pores (2.1 nm). The gene silencing effect of siRNA loaded ultra large pore MSNs was further confirmed in vitro and in vivo [118]. With large cavity in the core, hollow MSNs were supposed to have more space for siRNA loading compared to transitional MSNs. Chen et al. prepared hollow MSNs and further expanded the pore sizes from 3.2 nm to larger than 10 nm using a surfactant-directing alkaline-etching (SDAE) strategy. The hollow MSNs with large pore size have been demonstrated with higher siRNA-loading capabilities compared to HMSNs with small pores and effective siRNA intracellular transfection in vitro [106].

In light of the versatility of MSNs on drug delivery and release, some of the features such as active targeting and stimuli-responsive release can be also incorporated in MSNs based siRNA delivery system. Ashley et al. developed mesoporous silica nanoparticle supported lipid bilayers for siRNA delivery with multifunction. The MSNs core was loaded with siRNA and then grafted with liposomes on the outer surface. With the supported liposome bilayers on the surface, various functional molecules including PEG, targeting peptides and endosomolytic peptides can be attached. These so called “protocells” were able to specifically deliver siRNA into target cells and cause effective gene knock down on protein level [119]. Furthermore, the controlled intracellular release of siRNA from MSNs can be a promising way to protect siRNA from premature release in the physiological environment. Taratula and co-workers developed a MSNs based siRNA delivery system for inhalation treatment of lung cancer. siRNA targeting Pgp and Bcl-2 were attached to the surface of MSNs through disulphide bond which can be cleaved by redox in the cytoplasm [120]. Similar mechanism of siRNA released from MSNs that relied on disulphide bond cleavage was designed by Ma et al [121]. However, the siRNA was not connected with MSNs directly but attached to adamantane and ethylenediamine-modified β-cyclodextrin that were grafted on MSNs by disulphide bond to protect encapsulated Dox in pores from premature release. The intracellular acidic environment has also been explored as a trigger to activate the release of siRNA from MSNs [110].

5 Characterization and analysis via computer aided strategies

5.1 Determination of the surface area, pore geometry and pore size of MSNs

Large surface area, controllable pore geometry and pore size are advantageous properties of MSNs as drug carriers for targeted delivery. Depending on the physical characteristics of MSNs, several models were used to determine the surface area of MSNs, like Brunauer-Emmett-Teller (BET) method [122-127], Langmuir calculation and t-Plot calculation [128, 129]. The BET calculation obtains the sample surface area value by determining the monolayer volume of adsorbed gas from the isotherm data. The Langmuir calculation determines the surface area of a sample by relating the surface area to the volume of gas adsorbed as a monolayer. The t-Plot calculation allows quantitative analysis of the area and total volume ascribed to micropores. Matrix area, the area external to micropores, is directly determined by this method. Thus, t-Plot calculation often proves to be a valuable way of characterizing MSNs with microporosity and mesoporosity [130, 131]. Software such as MicroActive is widely used for these calculations.

According to the types of pores that define the networks, MSNs are divided into several types, such as Mobil Crystalline Materials (MCM-41) and Santa Barbara Amorphous type (SBA-16) [132]. Owning to different pore structure, the way of gas evaporation differs from one another, which results in the change in shape of the hysteresis loops on nitrogen adsorption-desorption isotherms (Figure 11) [133-135]. Sarkisov and Monson [134] studied the gas adsorption and desorption in pores with different pore geometries using computer graphics visualization. It was found that for the ink bottle geometry the large pore can empty during desorption even while the small pore remains filled with fluid.

The pore size of MSNs can be investigated by a suite of characterization techniques, such as Brunauer-Emmett-Teller/Barrett-Joyner-Halenda (BET/BJH), X-ray diffraction (XRD) and Positron Annihilation Lifetime Spectroscopy (PALS). These techniques provide different information whilst are complementary to each other. Morishige and Tateishi calculated the pore size of the ordered mesoporous MCM-41 and SBA-15 and found that a macroscopic thermodynamic approach based on Broekhoff-de Boer equations was in fair agreement with the experimental relation in their study [136].

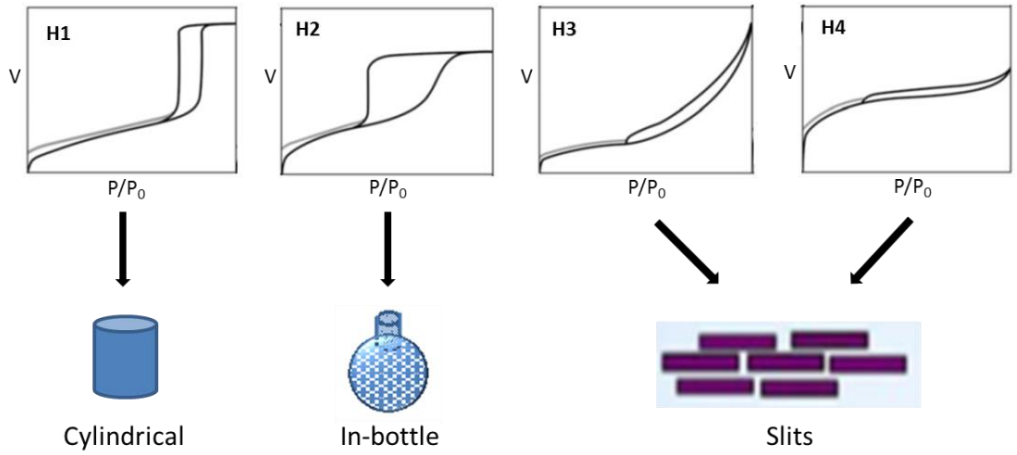

Figure 11 Effect of pore geometry on shapes of hysteresis loop. H1-H4: types of hysteresis loops

5.2 drug delivery kinetics

In the attempt to investigate the release kinetics of MSNs based drug delivery systems, equations and models [137, 138] were developed to describe the release behavior of these systems. For example, Eq. 1 was introduced by Ritger and Peppas for description of solute release from non-swellable and swellable devices in controlled release systems [139, 140],

$$\frac{Mt}{M\infty} = Kt^n \qquad (1)$$

where M_t/M_∞ is the accumulative release percentage of drug at time *t*; *k* is a constant and *n* is the diffusional exponent indicating the transport mechanism of the drug from their carriers. Table 1 lists the diffusional exponent values (*n*) and their corresponding drug release mechanism based on literature [141, 142]. Besides, Doadrio and co-workers constructed a molecular model to investigate the release behaviour of Chicago Sky Blue 6B from SBA-15 by molecular modelling calculations [143]. According to this model, the controlled release mechanism of SBA-15 functionalized with 3-aminopropyl-triethoxy-silane was fully explained. Similarly, the drug dissolution kinetics from ordered mesoporous silica MCM-41 and SBA-15 were modelled by Murzin and co-workers [144]. In their study, a simple model with two adjustable parameters was built to explain the Sigmoidal Behaviour of drug dissolution. Several

models have been introduced to interpret the release kinetics of cephalosporin from functionalized MCM-41 [145]. The correlations between the delivery rate and the surface properties of MCM-41 were successfully reflected by model parameters.

Table 1 Values of diffusional exponent and corresponding drug release mechanism

Diffusional exponent, n			Drug release mechanism
Thin film	Cylindrical samples	Spherical samples	
< 0.50	< 0.45	< 0.43	Quasi-Fickian diffusion
0.50	0.45	0.43	Fickian diffusion
0.50< n < 1.00	0.45 < n < 1.00	0.43 < n < 1.00	Non-Fickian diffusion (Anomalous transport)
1.00	1.00	1.00	Zero-order release

6 Perspectives and concluding remarks

The studies reported in this review established MSNs as a smart drug carrier that effectively transports drug/genes to the targeted cell population, but challenges remain for these MSNs based drug delivery systems to be further advanced and available for clinical purposes. For example, although modifications have made MSNs more versatile for applications, they also have disadvantages to be exploited as drug carriers. Firstly, if not well controlled, surface modifications of MSNs would cause structure collapse [26]. Further, the introduction of chemical groups on the surface of MSNs may create additional toxicity which makes MSNs unsuitable as carriers for drug delivery systems. Moreover, in many cases, it is difficult to couple several functional groups with sufficient concentration, since the number of active attachment sites on the particle surface is limited. In addition, each functionalization step might negatively affect the suspension stability of the particulate system, depending on the physicochemical properties of the added function. Therefore, all these issues should be considered when a drug delivery system is engineered based on modified MSNs and the development of effective methods to deal with these problems is of great importance.

References:

1. Kresge, C.T., et al., *Ordered mesoporous molecular sieves synthesized by a liquid-crystal template mechanism.* Nature, 1992. **359**(6397): p. 710-712.
2. Choi, Y.L., et al., *Controlled release using mesoporous silica nanoparticles functionalized with 18-crown-6 derivative.* Journal of Materials Chemistry, 2011. **21**(22): p. 7882-7885.
3. Radu, D.R., et al., *Gatekeeping Layer Effect: A Poly(lactic acid)-coated Mesoporous Silica Nanosphere-Based Fluorescence Probe for Detection of Amino-Containing Neurotransmitters.* Journal of the American Chemical Society, 2004. **126**(6): p. 1640-1641.
4. Mercier, L. and T.J. Pinnavaia, *Access in mesoporous materials: Advantages of a uniform pore structure in the design of a heavy metal ion adsorbent for environmental remediation.* Advanced Materials, 1997. **9**(6): p. 500-503.
5. Corma, A., *From microporous to mesoporous molecular sieve materials and their use in catalysis.* Chemical Reviews, 1997. **97**(6): p. 2373-2419.
6. Lu, J., et al., *Biocompatibility, biodistribution, and drug-delivery efficiency of mesoporous silica nanoparticles for cancer therapy in animals.* Small, 2010. **6**(16): p. 1794-805.
7. Slowing, I.I., et al., *Mesoporous silica nanoparticles: Structural design and applications.* Journal of Materials Chemistry, 2010. **20**(37): p. 7924-7937.
8. Mamaeva, V., et al., *Mesoporous Silica Nanoparticles as Drug Delivery Systems for Targeted Inhibition of Notch Signaling in Cancer.* Molecular Therapy, 2011. **19**(8): p. 1538-1546.
9. Lu, G.Q. and X.S. Zhao, *Nanoporous Materials - Science and Engineering*. 2004, United Kingdom: Imperial College Press.
10. Blin, J.L. and M. Imperor-Clerc, *Mechanism of Self-Assembly in The Synthesis Of Silica Mesoporous Materials: In Situ Studies by X-ray and Neutron Scattering.* Chemical Society Reviews, 2013. **42**(9): p. 4071-4082.

11. Yi, Z., et al., *A New Insight into Growth Mechanism and Kinetics of Mesoporous Silica Nanoparticles by in Situ Small Angle X-ray Scattering.* Langmuir, 2015. **31** (30): p. 8478–8487
12. Zhao, D.Y., et al., *Triblock Copolymer Syntheses of Mesoporous Silica with Periodic 50 to 300 Angstrom Pores.* Science, 1998. **279**: p. 548-552.
13. Huo, Q., D.I. Margolese, and G.D. Stucky, *Surfactant Control of Phases in the Synthesis of Mesoporous Silica-Based Materials.* Chemistry of Materials, 1996. **8**(5): p. 1147-1160.
14. Han, L., et al., *Synthesis of amino group functionalized monodispersed mesoporous silica nanospheres using anionic surfactant.* Microporous and Mesoporous Materials, 2011. **139**(1-3): p. 94-103.
15. Liu, Y., H. Miyoshi, and M. Nakamura, *Novel drug delivery system of hollow mesoporous silica nanocapsules with thin shells: Preparation and fluorescein isothiocyanate (FITC) release kinetics.* Colloids and Surfaces B: Biointerfaces, 2007. **58**(2): p. 180-187.
16. Ha, T.-J., et al., *Investigation of the effect of calcination temperature on HMDS-treated ordered mesoporous silica film.* Journal of Colloid and Interface Science, 2008. **326**(1): p. 186-190.
17. Beck, J.S., et al., *A new family of mesoporous molecular sieves prepared with liquid crystal templates.* Journal of the American Chemical Society, 1992. **114**(27): p. 10834-10843.
18. Huh, S., et al., *Organic Functionalization and Morphology Control of Mesoporous Silicas via a Co-Condensation Synthesis Method.* Chemistry of Materials, 2003. **15**(22): p. 4247-4256.
19. Chen, D., et al., *Facile and scalable synthesis of tailored silica "nanorattle" structures.* Advanced Materials, 2009. **21**(37): p. 3804-3807+3724.
20. Gao, H., W. Shi, and L.B. Freund, Proc. Natl. Acad. Sci., 2005. **302**: p. 94699474.
21. Vivero-Escoto, J.L., et al., *Mesoporous silica nanoparticles for intracellular controlled drug delivery.* Small, 2010. **6**(18): p. 1952-1967.

22. Li, Y., et al., *Hollow spheres of mesoporous aluminosilicate with a three-dimensional pore network and extraordinarily high hydrothermal stability.* Nano Letters, 2003. **3**(5): p. 609-612.
23. Tang, F., L. Li, and D. Chen, *Mesoporous silica nanoparticles: Synthesis, biocompatibility and drug delivery.* Advanced Materials, 2012. **24**(12): p. 1504-1534.
24. Guo, Y., et al., *Chitosan-g-TPGS nanoparticles for anticancer drug delivery and overcoming multidrug resistance.* Molecular Pharmaceutics, 2014. **11**(1): p. 59-70.
25. Feng, Z., et al., *A facile route to hollow nanospheres of mesoporous silica with tunable size.* Chemical Communications, 2008(23): p. 2629-2631.
26. Kao, K.C., C.J. Tsou, and C.Y. Mou, *Collapsed (kippah) hollow silica nanoparticles.* Chemical Communications, 2012. **48**(28): p. 3454-3456.
27. Mandal, M. and M. Kruk, *Family of single-micelle-templated organosilica hollow nanospheres and nanotubes synthesized through adjustment of organosilica/surfactant ratio.* Chemistry of Materials, 2012. **24**(1): p. 123-132.
28. Mei, X., et al., *Hollow mesoporous silica nanoparticles conjugated with pH-sensitive amphiphilic diblock polymer for controlled drug release.* Microporous and Mesoporous Materials, 2012. **152**: p. 16-24.
29. Zhang, T., et al., *Formation of hollow silica colloids through a spontaneous dissolution-regrowth process.* Angewandte Chemie - International Edition, 2008. **47**(31): p. 5806-5811.
30. Lou, X.W., L.A. Archer, and Z. Yang, *Hollow micro-/nanostructures: Synthesis and applications.* Advanced Materials, 2008. **20**(21): p. 3987-4019.
31. Chen, Y., et al., *Hollow/rattle-type mesoporous nanostructures by a structural difference-based selective etching strategy.* ACS Nano, 2010. **4**(1): p. 529-539.
32. Gao, Y., et al., *Controlled intracellular release of doxorubicin in multidrug-resistant cancer cells by tuning the shell-pore sizes of mesoporous silica nanoparticles.* ACS Nano, 2011. **5**(12): p. 9788-9798.
33. Zhang, Q., et al., *Permeable silica shell through surface-protected etching.* Nano Letters, 2008. **8**(9): p. 2867-2871.

34. He, Q., et al., *An anti-ROS/hepatic fibrosis drug delivery system based on salvianolic acid B loaded mesoporous silica nanoparticles.* Biomaterials, 2010. **31**(30): p. 7785-7796.

35. Lu, J., et al., *Mesoporous silica nanoparticles as a delivery system for hydrophobic anticancer drugs.* Small, 2007. **3**(8): p. 1341-1346.

36. Ramírez, A., et al., *Formation of Si-H groups during the functionalization of mesoporous silica with Grignard reagents.* Microporous and Mesoporous Materials, 2007. **98**(1-3): p. 115-122.

37. Manzano, M., et al., *Studies on MCM-41 mesoporous silica for drug delivery: Effect of particle morphology and amine functionalization.* Chemical Engineering Journal, 2008. **137**(1): p. 30-37.

38. Al Othman, Z. and A.W. Apblett, *Synthesis of mesoporous silica grafted with 3-glycidoxypropyltrimethoxy-silane.* Materials Letters, 2009. **63**(27): p. 2331-2334.

39. Ritter, H., et al., *A comparative study of the functionalization of mesoporous silica MCM-41 by deposition of 3-aminopropyltrimethoxysilane from toluene and from the vapor phase.* Microporous and Mesoporous Materials, 2009. **121**(1-3): p. 79-83.

40. Shen, C., et al., *Physicochemical properties of poly(ethylene oxide)-based composite polymer electrolytes with a silane-modified mesoporous silica SBA-15.* Electrochimica Acta, 2009. **54**(12): p. 3490-3494.

41. Liu, R., et al., *pH-Responsive Nanogated Ensemble Based on Gold-Capped Mesoporous Silica through an Acid-Labile Acetal Linker.* Journal of the American Chemical Society, 2010. **132**(5): p. 1500-1501.

42. Bajpai, A.K., et al., *Responsive polymers in controlled drug delivery.* Progress in Polymer Science, 2008. **33**(11): p. 1088-1118.

43. Torney, F., et al., *Mesoporous Silica Nanoparticles Deliver DNA and Chemicals into Plants.* Nature Nanotechnology, 2007. **2**(5): p. 295-300.

44. Du, L., H. Song, and S. Liao, *A biocompatible drug delivery nanovalve system on the surface of mesoporous nanoparticles.* Microporous and Mesoporous Materials, 2012. **147** (1): p. 200-204

45. Kim, H., et al., *Glutathione-Induced Intracellular Release of Guests from Mesoporous Silica Nanocontainers with Cyclodextrin Gatekeepers.* Advanced Materials, 2010. **22**(38): p. 4280-4283.

46. Lai, C.-Y., et al., *A Mesoporous Silica Nanosphere-Based Carrier System with Chemically Removable CdS Nanoparticle Caps for Stimuli-Responsive Controlled Release of Neurotransmitters and Drug Molecules.* Journal of the American Chemical Society, 2003. **125**(15): p. 4451-4459.

47. Li, H., et al., *Near-Infrared Light-Responsive Supramolecular Nanovalve Based on Mesoporous Silica-Coated Gold Nanorods.* Chemical Science, 2014. **5**(7): p. 2804-2808.

48. Zhang, Z., et al., *Mesoporous Silica-Coated Gold Nanorods as a Light-Mediated Multifunctional Theranostic Platform for Cancer Treatment.* Advanced Materials, 2012. **24**(11): p. 1418-1423.

49. Niu, N., et al., *Up-Conversion Nanoparticle Assembled Mesoporous Silica Composites: Synthesis, Plasmon-Enhanced Luminescence, and Near-Infrared Light Triggered Drug Release.* ACS Applied Materials & Interfaces, 2014. **6**(5): p. 3250-3262.

50. Yi, Z., et al., *Functionalized Mesoporous Silica Nanoparticles with Redox-Responsive Short-Chain Gatekeepers for Agrochemical Delivery.* ACS Appl Mater Interfaces, 2015. **7**(18): p. 9937-46.

51. Zhu, Y., et al., *PEGylated hollow mesoporous silica nanoparticles as potential drug delivery vehicles.* Microporous and Mesoporous Materials, 2011. **141**(1-3): p. 199-206.

52. Niu, D., et al., *Synthesis of Core−Shell Structured Dual-Mesoporous Silica Spheres with Tunable Pore Size and Controllable Shell Thickness.* Journal of the American Chemical Society, 2010. **132**(43): p. 15144-15147.

53. Fang, J., H. Nakamura, and H. Maeda, *The EPR effect: Unique features of tumor blood vessels for drug delivery, factors involved, and limitations and augmentation of the effect.* Advanced Drug Delivery Reviews, 2011. **63**(3): p. 136-151.

54. Mamaeva, V., et al., *Mesoporous Silica Nanoparticles as Drug Delivery Systems for Targeted Inhibition of Notch Signaling in Cancer.* Mol Ther, 2011. **19**(8): p. 1538-1546.

55. Shen, J., et al., *Mesoporous silica nanoparticles loading doxorubicin reverse multidrug resistance: performance and mechanism.* Nanoscale, 2011. **3**(10): p. 4314-22.

56. Meng, H., et al., *Use of size and a copolymer design feature to improve the biodistribution and the enhanced permeability and retention effect of doxorubicin-loaded mesoporous silica nanoparticles in a murine xenograft tumor model.* ACS Nano, 2011. **5**(5): p. 4131-44.

57. Chen, F., et al., *Engineering of hollow mesoporous silica nanoparticles for remarkably enhanced tumor active targeting efficacy.* Sci Rep, 2014. **4**: p. 5080.

58. de Barros, A.L., et al., *Synthesis, characterization, and biodistribution studies of (99m)Tc-labeled SBA-16 mesoporous silica nanoparticles.* Mater Sci Eng C Mater Biol Appl, 2015. **56**: p. 181-8.

59. Maldiney, T., et al., *Mesoporous persistent nanophosphors for in vivo optical bioimaging and drug-delivery.* Nanoscale, 2014. **6**(22): p. 13970-6.

60. Miller, L., et al., *Synthesis, characterization, and biodistribution of multiple 89Zr-labeled pore-expanded mesoporous silica nanoparticles for PET.* Nanoscale, 2014. **6**(9): p. 4928-35.

61. Chen, F., et al., *In Vivo Tumor Vasculature Targeting of CuS@MSN Based Theranostic Nanomedicine.* ACS Nano, 2015. **9**(4): p. 3926-34.

62. Liu, T., et al., *Single and repeated dose toxicity of mesoporous hollow silica nanoparticles in intravenously exposed mice.* Biomaterials, 2011. **32**(6): p. 1657-68.

63. He, Q., et al., *In vivo biodistribution and urinary excretion of mesoporous silica nanoparticles: Effects of particle size and PEGylation.* Small, 2011. **7**(2): p. 271-280.

64. Huang, X., et al., *The shape effect of mesoporous silica nanoparticles on biodistribution, clearance, and biocompatibility in vivo.* ACS Nano, 2011. **5**(7): p. 5390-5399.

65. Souris, J.S., et al., *Surface charge-mediated rapid hepatobiliary excretion of mesoporous silica nanoparticles.* Biomaterials, 2010. **31**(21): p. 5564-5574.

66. Xie, M., et al., *Negative-charge-functionalized mesoporous silica nanoparticles as drug vehicles targeting hepatocellular carcinoma.* Int J Pharm, 2014. **474**(1-2): p. 223-31.

67. Yu, T., et al., *In vivo biodistribution and pharmacokinetics of silica nanoparticles as a function of geometry, porosity and surface characteristics.* J Control Release, 2012. **163**(1): p. 46-54.

68. Canton, I. and G. Battaglia, *Endocytosis at the nanoscale.* Chemical Society Reviews, 2012. **41**(7): p. 2718-2739.

69. Vivero-Escoto, J.L., et al., *Mesoporous Silica Nanoparticles for Intracellular Controlled Drug Delivery.* Small, 2010. **6**(18): p. 1952-1967.

70. Iversen, T.-G., T. Skotland, and K. Sandvig, *Endocytosis and intracellular transport of nanoparticles: Present knowledge and need for future studies.* Nano Today, 2011. **6**(2): p. 176-185.

71. Slowing, I., B.G. Trewyn, and V.S.Y. Lin, *Effect of Surface Functionalization of MCM-41-Type Mesoporous Silica Nanoparticles on the Endocytosis by Human Cancer Cells.* Journal of the American Chemical Society, 2006. **128**(46): p. 14792-14793.

72. Sun, W., et al., *Endocytosis of a single mesoporous silica nanoparticle into a human lung cancer cell observed by differential interference contrast microscopy.* Analytical and Bioanalytical Chemistry, 2008. **391**(6): p. 2119-2125.

73. He, Q., et al., *Intracellular Localization and Cytotoxicity of Spherical Mesoporous Silica Nano- and Microparticles.* Small, 2009. **5**(23): p. 2722-2729.

74. Chen, Y., et al., *Manganese oxide-based multifunctionalized mesoporous silica nanoparticles for pH-responsive MRI, ultrasonography and circumvention of MDR in cancer cells.* Biomaterials, 2012. **33**(29): p. 7126-37.

75. Lu, F., et al., *Size Effect on Cell Uptake in Well-Suspended, Uniform Mesoporous Silica Nanoparticles.* Small, 2009. **5**(12): p. 1408-1413.

76. Gan, Q., et al., *Effect of size on the cellular endocytosis and controlled release of mesoporous silica nanoparticles for intracellular delivery.* Biomed Microdevices, 2012. **14**(2): p. 259-70.

77. Ekkapongpisit, M., et al., *Biocompatibility, endocytosis, and intracellular trafficking of mesoporous silica and polystyrene nanoparticles in ovarian cancer cells: effects of size and surface charge groups.* Int J Nanomedicine, 2012. **7**: p. 4147-58.

78. Zhu, J., et al., *Ultrasmall, Well-Dispersed, Hollow Siliceous Spheres with Enhanced Endocytosis Properties.* Small, 2010. **6**(2): p. 276-282.

79. Chung, T.H., et al., *The effect of surface charge on the uptake and biological function of mesoporous silica nanoparticles in 3T3-L1 cells and human mesenchymal stem cells.* Biomaterials, 2007. **28**(19): p. 2959-66.

80. Wang, J., et al., *Increasing cellular uptake of mesoporous silica nanoparticles in human embryonic kidney cell line 293T cells by using Lipofectamine 2000.* J Biomed Nanotechnol, 2013. **9**(11): p. 1882-90.

81. Trewyn, B.G., et al., *Biocompatible mesoporous silica nanoparticles with different morphologies for animal cell membrane penetration.* Chemical Engineering Journal, 2008. **137**(1): p. 23-29.

82. Gao, H., W. Shi, and L.B. Freund, *Mechanics of receptor-mediated endocytosis.* Proceedings of the National Academy of Sciences of the United States of America, 2005. **102**(27): p. 9469-74.

83. Huang, X., et al., *The effect of the shape of mesoporous silica nanoparticles on cellular uptake and cell function.* Biomaterials, 2010. **31**(3): p. 438-48.

84. He, Q. and J. Shi, *Mesoporous silica nanoparticle based nano drug delivery systems: synthesis, controlled drug release and delivery, pharmacokinetics and biocompatibility.* Journal of Materials Chemistry, 2011. **21**(16): p. 5845-5855.

85. Rosenholm, J.M., et al., *Targeting of porous hybrid silica nanoparticles to cancer cells.* ACS Nano, 2009. **3**(1): p. 197-206.

86. Pang, J., et al., *Folate-conjugated hybrid SBA-15 particles for targeted anticancer drug delivery.* J Colloid Interface Sci, 2013. **395**: p. 31-9.

87. Wittig, R., et al., *Active targeting of mesoporous silica drug carriers enhances gamma-secretase inhibitor efficacy in an in vivo model for breast cancer*. Nanomedicine (Lond), 2014. **9**(7): p. 971-87.

88. Luo, Z., et al., *Engineering a hollow nanocontainer platform with multifunctional molecular machines for tumor-targeted therapy in vitro and in vivo.* ACS Nano, 2013. **7**(11): p. 10271-84.

89. Mohapatra, S., et al., *Multifunctional mesoporous hollow silica nanocapsules for targeted co-delivery of cisplatin-pemetrexed and MR imaging.* Dalton Trans, 2014. **43**(42): p. 15841-50.
90. Ma, X., Q. Qu, and Y. Zhao, *Targeted delivery of 5-aminolevulinic acid by multifunctional hollow mesoporous silica nanoparticles for photodynamic skin cancer therapy.* ACS Appl Mater Interfaces, 2015. **7**(20): p. 10671-6.
91. Chen, Z., et al., *Bioresponsive hyaluronic acid-capped mesoporous silica nanoparticles for targeted drug delivery.* Chemistry, 2013. **19**(5): p. 1778-83.
92. Yu, M., et al., *Hyaluronic acid modified mesoporous silica nanoparticles for targeted drug delivery to CD44-overexpressing cancer cells.* Nanoscale, 2013. **5**(1): p. 178-83.
93. Zhao, Q., et al., *Dual-stimuli responsive hyaluronic acid-conjugated mesoporous silica for targeted delivery to CD44-overexpressing cancer cells.* Acta Biomater, 2015. **23**: p. 147-56.
94. Zhao, Q., et al., *Hyaluronic acid oligosaccharide modified redox-responsive mesoporous silica nanoparticles for targeted drug delivery.* ACS Appl Mater Interfaces, 2014. **6**(22): p. 20290-9.
95. He, Q., et al., *Mesoporous carbon@silicon-silica nanotheranostics for synchronous delivery of insoluble drugs and luminescence imaging.* Biomaterials, 2012. **33**(17): p. 4392-402.
96. Sundarraj, S., et al., *Ligand-conjugated mesoporous silica nanorattles based on enzyme targeted prodrug delivery system for effective lung cancer therapy.* Toxicol Appl Pharmacol, 2014. **275**(3): p. 232-43.
97. She, X., et al., *The control of epidermal growth factor grafted on mesoporous silica nanoparticles for targeted delivery.* Journal of Materials Chemistry B, 2015. **3**(29): p. 6094-6104.
98. She, X., et al., *Fabrication of high specificity hollow mesoporous silica nanoparticles assisted by Eudragit for targeted drug delivery.* Journal of Colloid and Interface Science, 2015. **445**(0): p. 151-160.

99. Chen, L., et al., *Overcoming acquired drug resistance in colorectal cancer cells by targeted delivery of 5-FU with EGF grafted hollow mesoporous silica nanoparticles.* Nanoscale, 2015. **7**(33): p. 14080-14092.

100. Fire, A., et al., *Potent and specific genetic interference by double-stranded RNA in Caenorhabditis elegans.* Nature, 1998. **391**(6669): p. 806-811.

101. de Fougerolles, A., et al., *Interfering with disease: a progress report on siRNA-based therapeutics.* Nat Rev Drug Discov, 2007. **6**(6): p. 443-453.

102. Silva, R., et al., *Modulation of P-glycoprotein efflux pump: induction and activation as a therapeutic strategy.* Pharmacology & Therapeutics, 2015. **149**: p. 1-123.

103. Xia, T., et al., *Polyethyleneimine Coating Enhances the Cellular Uptake of Mesoporous Silica Nanoparticles and Allows Safe Delivery of siRNA and DNA Constructs.* ACS Nano, 2009. **3**(10): p. 3273-3286.

104. Meng, H., et al., *Engineered design of mesoporous silica nanoparticles to deliver doxorubicin and P-glycoprotein siRNA to overcome drug resistance in a cancer cell line.* ACS Nano, 2010. **4**(8): p. 4539-50.

105. Meng, H., et al., *Codelivery of an Optimal Drug/siRNA Combination Using Mesoporous Silica Nanoparticles To Overcome Drug Resistance in Breast Cancer in Vitro and in Vivo.* ACS Nano, 2013. **7**(2): p.994-1005

106. Chen, Y., et al., *Reversible Pore-Structure Evolution in Hollow Silica Nanocapsules: Large Pores for siRNA Delivery and Nanoparticle Collecting.* Small, 2011. **7**(20): p. 2935-2944.

107. Hartono, S.B., et al., *Synthesis of multi-functional large pore mesoporous silica nanoparticles as gene carriers.* Nanotechnology, 2014. **25**(5): p. 055701.

108. Hom, C., et al., *Mesoporous silica nanoparticles facilitate delivery of siRNA to shutdown signaling pathways in mammalian cells.* Small, 2010. **6**(11): p. 1185-90.

109. Li, X., et al., *A mesoporous silica nanoparticle – PEI – Fusogenic peptide system for siRNA delivery in cancer therapy.* Biomaterials, 2013. **34**(4): p. 1391-1401.

110. Ma, X., et al., *Integrated Hollow Mesoporous Silica Nanoparticles for Target Drug/siRNA Co-Delivery.* Chemistry – A European Journal, 2013. **19**(46): p. 15593-15603.

111. Shen, J., et al., *Cyclodextrin and Polyethylenimine Functionalized Mesoporous Silica Nanoparticles for Delivery of siRNA Cancer Therapeutics.* Theranostics, 2014. **4**(5): p. 487-97.

112. Chen, A.M., et al., *Co-delivery of Doxorubicin and Bcl-2 siRNA by Mesoporous Silica Nanoparticles Enhances the Efficacy of Chemotherapy in Multidrug-Resistant Cancer Cells.* Small, 2009. **5**(23): p. 2673-2677.

113. Bhattarai, S.R., et al., *Enhanced gene and siRNA delivery by polycation-modified mesoporous silica nanoparticles loaded with chloroquine.* Pharmaceutical research, 2010. **27**(12): p. 2556-68.

114. Hartono, S.B., et al., *Poly-l-lysine Functionalized Large Pore Cubic Mesostructured Silica Nanoparticles as Biocompatible Carriers for Gene Delivery.* ACS Nano, 2012. **6**(3): p. 2104-2117.

115. Li, X., et al., *The packaging of siRNA within the mesoporous structure of silica nanoparticles.* Biomaterials, 2011. **32**(35): p. 9546-9556.

116. Chen, Y., et al., *Highly effective inhibition of lung cancer growth and metastasis by systemic delivery of siRNA via multimodal mesoporous silica-based nanocarrier.* Biomaterials, 2014. **35**(38): p. 10058-69.

117. Chen, Y., et al., *Highly effective antiangiogenesis via magnetic mesoporous silica-based siRNA vehicle targeting the VEGF gene for orthotopic ovarian cancer therapy.* International Journal of Nanomedicine, 2015. **10**: p. 2579-2594.

118. Na, H.K., et al., *Efficient functional delivery of siRNA using mesoporous silica nanoparticles with ultralarge pores.* Small, 2012. **8**(11): p. 1752-61.

119. Ashley, C.E., et al., *Delivery of Small Interfering RNA by Peptide-Targeted Mesoporous Silica Nanoparticle-Supported Lipid Bilayers.* ACS Nano, 2012. **6**(3): p. 2174-2188.

120. Taratula, O., et al., *Innovative strategy for treatment of lung cancer: targeted nanotechnology-based inhalation co-delivery of anticancer drugs and siRNA.* Journal of Drug Targeting, 2011. **19**(10): p. 900-914.

121. Ma, X., et al., *Redox-Responsive Mesoporous Silica Nanoparticles: A Physiologically Sensitive Codelivery Vehicle for siRNA and Doxorubicin.* Antioxid Redox Signal, 2014. **21**(5): p.707-722

122. Ladavos, A.K., et al., *The BET equation, the inflection points of N 2 adsorption isotherms and the estimation of specific surface area of porous solids.* Microporous and Mesoporous Materials, 2012. **151**: p. 126-133.

123. Blas, H., et al., *Elaboration of monodisperse spherical hollow particles with ordered mesoporous silica shells via dual latex/surfactant templating: Radial orientation of mesopore channels.* Langmuir, 2008. **24**(22): p. 13132-13137.

124. Franke, O., et al., *Unusual type of adsorption isotherm describing capillary condensation without hysteresis.* Journal of the Chemical Society, Chemical Communications, 1993(9): p. 724-726.

125. Branton, P.J., et al., *Physisorption of argon, nitrogen and oxygen by MCM-41, a model mesoporous adsorbent.* Journal of the Chemical Society, Faraday Transactions, 1994. **90**(19): p. 2965-2967.

126. Branton, P.J., P.G. Hall, and K.S.W. Sing, *Physisorption of nitrogen and oxygen by MCM-41, a model mesoporous adsorbent.* Journal of the Chemical Society, Chemical Communications, 1993(16): p. 1257-1258.

127. Huang, X., N.P. Young, and H.E. Townley, *Characterization and comparison of mesoporous silica particles for optimized drug delivery.* Nanomaterials and Nanotechnology, 2014. **4**(2). DOI: 10.5772/58290

128. Jaroniec, M., M. Kruk, and J.P. Olivier, *Standard nitrogen adsorption data for characterization of nanoporous silicas.* Langmuir, 1999. **15**(16): p. 5410-5413.

129. Jaroniec, M. and P.F. Fulvio, *Standard nitrogen adsorption data for α-alumina and their use for characterization of mesoporous alumina-based materials.* Adsorption, 2013. **19**(2-4): p. 475-481.

130. Naik, S.P., et al., *Formation of silicalite-1 hollow spheres by the self-assembly of nanocrystals.* Chemistry of Materials, 2003. **15**(3): p. 787-792.

131. Hu, J., et al., *A facile and general fabrication method for organic silica hollow spheres and their excellent adsorption properties for heavy metal ions.* Journal of Materials Chemistry A, 2014. **2**(46): p. 19771-19777.

132. Shaobin, W., *Ordered mesoporous materials for drug delivery*. Microporous and Mesoporous Materials, 2009. **117**(1-2): p. 1-9.

133. Ravikovitch, P.I. and A.V. Neimark, *Experimental Confirmation of Different Mechanisms of Evaporation from Ink-Bottle Type Pores: Equilibrium, Pore Blocking, and Cavitation.* Langmuir, 2002. **18**(25): p. 9830-9837.

134. Sarkisov, L. and P.A. Monson, *Modeling of Adsorption and Desorption in Pores of Simple Geometry Using Molecular Dynamics.* Langmuir, 2001. **17**(24): p. 7600-7604.

135. Kruk, M. and M. Jaroniec, *Gas Adsorption Characterization of Ordered Organic−Inorganic Nanocomposite Materials.* Chemistry of Materials, 2001. **13**(10): p. 3169-3183.

136. Morishige, K. and M. Tateishi, *Accurate Relations between Pore Size and the Pressure of Capillary Condensation and the Evaporation of Nitrogen in Cylindrical Pores.* Langmuir, 2006. **22**(9): p. 4165-4169.

137. Maria, G., et al., *Kinetic studies on the irinotecan release based on structural properties of functionalized mesoporous-silica supports.* Microporous and Mesoporous Materials, 2012. **149**(1): p. 25-35.

138. Doadrio, A.L., et al., *A rational explanation of the vancomycin release from SBA-15 and its derivative by molecular modelling.* Microporous and Mesoporous Materials, 2010. **132**(3): p. 559-566.

139. Ritger, P.L. and N.A. Peppas, *A simple equation for desciption of solute release I. Fickian and non-Fickian release from non-swellable devices in the form of slabs, spheres, cylinders or discs.* Journal of Controlled Release, 1987. **5**(1): p. 23-36.

140. Ritger, P.L. and N.A. Peppas, *A simple equation for description of solute release II. Fickian and anomalous release from swellable devices.* Journal of Controlled Release, 1987. **5**(1): p. 37-42.

141. Salome, A.C., C.O. Godswill, and I.O. Ikechukwu, *Kinetics and mechanisms of drug release from swellable and non swellable matrices: A review.* Research Journal of Pharmaceutical, Biological and Chemical Sciences, 2013. **4**(2): p. 97-103.

142. Kosmidis, K., et al., *Analysis of Case II drug transport with radial and axial release from cylinders.* International Journal of Pharmaceutics, 2003. **254**(2): p. 183-188.

143. Doadrio, A.L., et al., *A molecular model to explain the controlled release from SBA-15 functionalized with APTES.* Microporous and Mesoporous Materials, 2014. **195**: p. 43-49.

144. Murzin, D.Y. and T. Heikkilä, *MODELING OF DRUG DISSOLUTION KINETICS WITH SIGMOIDAL BEHAVIOR FROM ORDERED MESOPOROUS SILICA.* Chemical Engineering Communications, 2014. **201**(5): p. 579-592.

145. Maria, G., et al., *Cephalosporin release from functionalized MCM-41 supports interpreted by various models.* Microporous and Mesoporous Materials, 2012. **162**: p. 80-90.